



(RESEARCH ARTICLE)



Basement depths estimation using the Euler-3D and source parameter imaging methods from the analysis of ground magnetic field data in the Niger Delta Basin

Princewill Nnamdi OKECHUKWU^{1,2,*}, Williams Nirorowan OFUYAH¹ and Ajirioghene Moses OGUH¹

¹ Department of Earth Science, Faculty of Science, Federal University of Petroleum Resources, Effurun, (FUPRE), Nigeria

² Three and Three Consult Limited, Abuja, Nigeria.

International Journal of Science and Research Archive, 2025, 14(01), 218-229

Publication history: Received on 27 October 2024; revised on 09 November 2024; accepted on 12 November 2024

Article DOI: <https://doi.org/10.30574/ijrsra.2025.14.1.2385>

Abstract

This study estimates basement depths in the Niger Delta Basin using ground magnetic field data, analysed through Euler-3D deconvolution and Source Parameter Imaging (SPI) methods. Ground magnetic data were collected with an AMC-6 High-precision Fluxgate Magnetometer across 6 dip and 14 strike profiles, alongside a tie-line. The Euler-3D deconvolution method was applied to map the depth and distribution of magnetic sources by solving Euler's homogeneity equation, while the SPI method provided an independent depth estimate using the local wavenumber approach. Both methods revealed significant basement depth variations that align with known structural features of the basin. This integrated analysis offers a robust interpretation of the subsurface architecture, enhancing the understanding of the region's geology and supporting ongoing resource exploration. The findings highlight the effectiveness of combining Euler-3D and SPI techniques for subsurface exploration in complex geological settings like the Niger Delta Basin.

Keywords: Euler-3d Deconvolution; Source Parameter Imaging; Ground magnetics; Depth estimation

1. Introduction

The use of magnetic field data in geophysical exploration, particularly in studying the tectonic structure of the upper crust, is well-established. Since basement rocks respond to magnetic fields, correlations between basement features and magnetic expressions are common. Magnetic and gravity data, when combined with modern analytical tools, can reveal the impact of tectonic history on sedimentary sections. These datasets can address key exploration questions, such as the location and depth of source rocks, sediment thickness, and tectonic influences on deposition [13, 19].

Magnetic exploration can also highlight major geologic lineation, tectonic structures, and the distribution of volcanic rocks. Patterns in regional aeromagnetic data can provide insights into the distribution of intrusive and extrusive rocks, as well as boundaries between magnetic terrains [14]. Additionally, frequency analysis is valuable in gravity and magnetic interpretation, simplifying complex geophysical problems through filter theory and allowing for a clearer understanding of data [8, 18, 23].

In sedimentary basins, like the Niger Delta, the method's effectiveness stems from the magnetization difference between the basement and sedimentary layers [21]. The use of enhanced techniques and 3D forward modelling has the potential to better elucidate the connection between basement features and hydrocarbon targets in such regions, though it remains underexplored in some areas, including the Niger Delta [4]. This study aims to analyse and map ground magnetic anomalies in the spectral domain in the low-latitude sedimentary terrain of Effurun.

* Corresponding author: Princewill Nnamdi OKECHUKWU

1.1. The Study Area

The study area is situated in the Niger Delta city of Effurun, at latitudes N5° 34' and longitude E005° 50', with an average elevation of about 8m above sea level. Sedimentary rock, including clay, sandstone, and shale, is the dominant rock type in this region.

The Tertiary Niger Delta comprises a regressive clastic succession, reaching up to 12,000 meters in thickness over approximately 75,000 square kilometres. Located in the Gulf of Guinea, it is one of the most productive hydrocarbon regions globally. The Niger Delta is bounded by the Anambra Basin and Abakaliki High to the north, the Cameroon volcanic line to the east, the Dahomey Embayment to the west, and the Gulf of Guinea to the south [2, 7]. Its siliciclastic system began progradation during the Late Eocene and continues today, forming three key lithostratigraphic units: the Akata, Agbada, and Benin formations [5, 11].

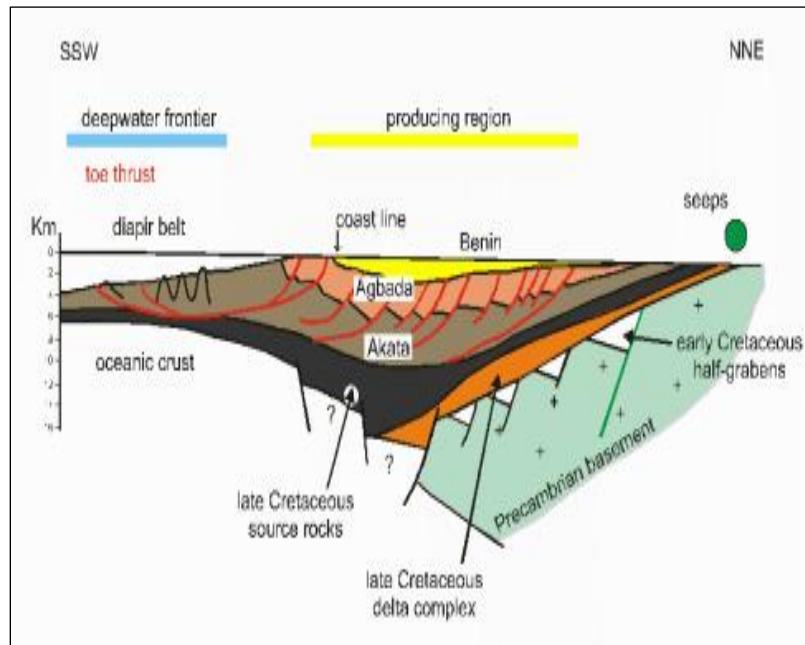


Figure 1 Averaged section of Niger Delta [24]

The Akata Formation is the basal unit which comprises over-pressured marine shales, sandy turbidites, and channel fills, deposited from the Late Eocene to the present. The Akata Formation, reaching thicknesses of up to 7,000 meters beneath the continental shelf, serves as a key source rock for hydrocarbons in the delta [7, 9, 26].

The Agbada Formation is the main petroleum-bearing unit of the Niger Delta, the Agbada Formation, consists of alternating sand and shale layers deposited in deltaic, paralic, and marine environments. With thicknesses exceeding 3,500 meters, it is divided into upper, middle, and lower units, with the middle unit being the primary target for hydrocarbon exploration due to its high sand content [7, 20].

The Benin Formation is an alluvial and coastal plain deposit up to 2,000 meters thick, overlying the Agbada Formation in onshore and coastal areas, ranging in age from the Late Eocene to the Recent [2].

The Niger Delta's structural framework is characterized by extensional, translational, and compressional domains along its continental margin. These domains exhibit growth faults, mud diapirism, and imbricate toe-of-slope thrusts, respectively, resulting from gravitational delta tectonics [6, 17]. The delta's continental shelf, about 50-80 km wide, transitions to the abyssal plains of the Gulf of Guinea, with water depths exceeding 4.5 km [24].

1.2. Source Parameter Imaging (SPI)

Source Parameter Imaging (SPI) is a technique used to estimate the depth and nature of subsurface magnetic sources directly from gridded magnetic data. It is particularly valuable in magnetic anomaly interpretation, providing a quick and efficient means of determining source depth without requiring complex modelling or inversion techniques.

SPI is based on the principle that magnetic anomalies can be analysed to determine the depth to the top of magnetic sources. The technique uses the local wavenumber, derived from the magnetic data, to estimate depth. The local wavenumber is a quantity that combines the horizontal and vertical gradients of the magnetic field.

The SPI method involves the following steps:

Calculation of the Analytical Signal: The analytical signal of the magnetic anomaly data is calculated. The analytical signal is a complex quantity that combines the original magnetic field data with its Hilbert transform.

Computation of Local Wavenumber: The local wavenumber k is computed using the horizontal and vertical derivatives of the magnetic field. The local wavenumber is given by:

$$k = \frac{1}{2\pi} \sqrt{\left(\frac{\partial T}{\partial x}\right)^2 + \left(\frac{\partial T}{\partial y}\right)^2} \dots\dots\dots(1)$$

The local wavenumber is proportional to the depth of the magnetic source, with higher wavenumbers indicating shallower sources.

Depth Estimation: The depth to the top of the magnetic source is estimated using the following relationship:

$$z = \frac{-1}{k} \dots\dots\dots(2)$$

Where z is the depth to the magnetic source; k is the local wavenumber.

This simple relationship allows for the depth to be estimated directly from the magnetic data without the need for iterative modelling.

Mapping and Interpretation: The SPI technique produces a depth map that shows the estimated depth to the top of magnetic sources across the survey area. This map can be used to identify structural features such as faults, intrusions, and other geological boundaries.

1.3. Standard Euler Deconvolution

Standard Euler Deconvolution is a widely used technique in geophysics for estimating the location and depth of magnetic and gravity sources from potential field data [22]. It is based on Euler's homogeneity equation, which relates the rate of change of the field with respect to distance to the depth of the source, allowing for the determination of source positions from the observed data.

Euler Deconvolution relies on the assumption that the magnetic or gravity field T and its gradients $\frac{\partial T}{\partial x}$, $\frac{\partial T}{\partial y}$, and $\frac{\partial T}{\partial z}$ satisfy the Euler's homogeneity equation. The equation for a magnetic or gravity anomaly is given by Reid et al., [22]:

$$(x - x_0) \frac{\partial T}{\partial x} + (y - y_0) \frac{\partial T}{\partial y} + (z - z_0) \frac{\partial T}{\partial z} = N(T - B) \dots\dots(4)$$

Where:

(x_0, y_0, z_0) are the coordinates of the magnetic or gravity source.

(x, y, z) are the coordinates where the field T is measured.

N is the structural index, which is a measure of the type of source (e.g., $N = 0$ for a contact, $N = 1$ for a dike, $N=2$ for a pipe, and so on).

B is the regional background field.

The goal of Euler Deconvolution is to solve this equation for the unknown source locations (x_0, y_0, z_0) . Euler Deconvolution provides an excellent tool for providing good depth estimations and locations of various sources in a given area, assuming that appropriate parameter selections are made.

Table 1 Structural Indices for Simple Models Used for Depth Estimations in 3D Euler Deconvolution [10]

Geological model	Number of Infinite Dimensions	Magnetic Structural Index
Sphere	0	3
Pipe	1 (z)	2
Horizontal cylinder	1 (x or y)	2
Dyke	2 (z and x or y)	1
Sill	2 (x and y)	1
Contact	3 (x, y and z)	0

Depending upon the potential source type, a structural index is chosen. This structural index is also a measure of the distinctive fall-off rate of the geologic feature. For example, the best results for a contact are obtained by structural indices of 0, while for thin two-dimensional dyke structures a structural index of 1 yields the best estimates, as explained in table 1. The number of infinite dimensions describes the extension of the geologic models in space.

2. Review of Previous Study

Kasidi & Nur [14] conducted a study of Jalingo and its surroundings using spectral analysis and Hilbert transformation of aeromagnetic data to estimate the depth of magnetic sources. Their analysis revealed two depth levels: deeper magnetic sources ranging from 437 m to 2617 m and shallow sources between 123 m and 436 m. Additionally, they estimated the Curie point depth to be between 24 km and 28 km, with a geothermal gradient of 21 °C/km –23 °C/km and heat flow values ranging from 53 mW/m² to 61 mW/m², indicating modest geothermal resources in the region. A notable inverse relationship was found between Curie depths and heat flow.

Similarly, Asielue et al. [1] interpreted aeromagnetic data from the Otukpo and Ejekwe areas of the lower Benue Trough using spectral analysis to determine basement depths. Their results showed two depth models: deep magnetic sources between 2546.5 m and 4177.3 m, averaging 3058 m, and shallow sources from 309.4 m to 762.5 m, averaging 527 m. They found that Otukpo had thicker sedimentary layers conducive to hydrocarbon accumulation, while Ejekwe had significant lateral intrusions indicative of older source rocks.

Tsepav & Mallam [25] analysed magnetic data from the Bida Basin, revealing shallow magnetic sources at depths ranging from 0.254 km to 1.719 km, with an average of 0.968 km. Deeper sources varied from 1.830 km to 4.615 km, averaging 3.063 km. The shallower sources were associated with near-surface ferruginous sandstones, ironstones, or laterites, while the deeper sources were linked to magnetic basement intrusions and structural features like dykes, faults, and horsts.

Hussaini et al. [12] processed high-resolution aeromagnetic data over northeastern Nigeria (sheet 84) using spectral analysis and found deeper magnetic sources ranging from 1948.3 m to 4503.9 m, with the deepest located in Katagum, Bauchi State. The shallow source map revealed that central and northern regions had the shallowest depths, while southern sections exhibited greater depths.

3. Material and methods

3.1. Data Acquisition

The field data for this research was collected using a man-borne surveying method, with the AMC-6 High-Precision Fluxgate Magnetometer employed to measure the vertical (Z) component of the geomagnetic field. The magnetometer, essential for recording magnetic variations, operates with a measurement range of 10,000 nT – 100,000 nT and a resolution of 0.1 nT –1 nT. Additionally, accessory tools like the Global Positioning System (GPS), measuring tapes, and hammers were used for determining coordinates, elevation, and other spatial data. The GPS provided the geographic coordinates and elevation for each survey station.

The study area was laid out in a grid with 14 lines trending NE-SW along the strike and 6 lines running E-W along the dip. Strike traverses were 50 meters long with 21 stations, spaced 5 meters apart, while the dip traverses extended 130 meters with 27 stations, also spaced 5 meters apart. The inter-line spacing was 10 meters for both orientations.

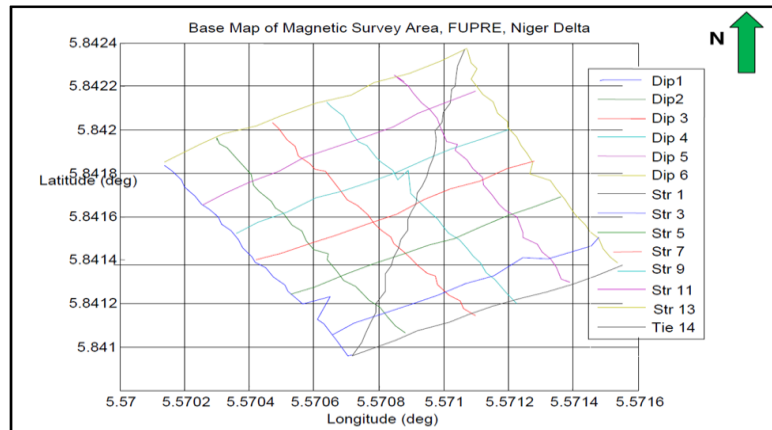


Figure 2 Abridged Base map showing 6 Dip lines, 7 Strike lines and 1 tie-line. A total of 14 Strike lines were recorded.

3.2. Data Processing

The raw magnetic data collected during the survey was first corrected for drift and diurnal variations to ensure accuracy. The vertical component of the geomagnetic field was then used to derive other components. To minimize the effects of magnetic inclination and declination, the corrected data was reduced to the equator (RTE), aligning the magnetic anomalies with their sources. This transformation used local geomagnetic parameters of -17.1° inclination and -3.2° declination. Various derivative techniques were then applied to the data, including First Vertical Derivative (FVD) to highlight shallow magnetic sources, Horizontal Gradient Magnitude (HGM) to map the edges of magnetic sources, and Analytical Signal Amplitude (ASA) to combine horizontal and vertical gradients for identifying magnetic bodies. Upward Continuation (UC) was also used to emphasize deeper geological features.

For depth estimation, two primary methods were applied: Source Parameter Imaging (SPI) and Standard Euler Deconvolution. SPI provided direct depth estimates of magnetic sources, which is crucial for interpreting the subsurface structure. The Euler Deconvolution method used the gradients of the magnetic field to estimate the depth and location of magnetic sources, offering further insights into the distribution of subsurface features. Together, these techniques and maps, generated from processed aeromagnetic data, offered a comprehensive view of the geological structures in the study area, revealing details about faults, contacts, and potential areas of interest for further exploration.

4. Results

Figure 4 shows the map of the vertical component of the geomagnetic field in the study area. The map shows the presence of highly magnetized bodies trending in the NW-SE direction. The vertical component magnetic intensity ranged from -5670.56nT to -14781.70nT with an average intensity of -10639.94nT .

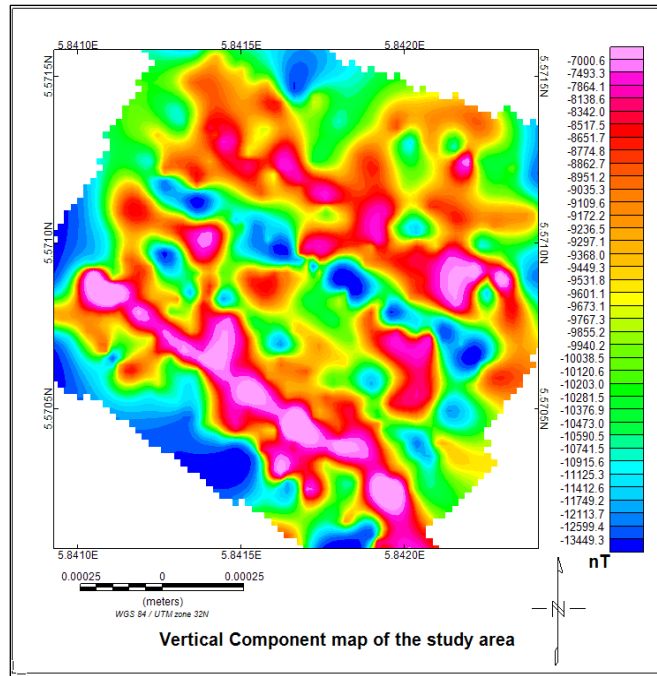


Figure 3 Map of the vertical component of the geomagnetic field.

4.1. Reduction To Equator Map

The RTE map of the study area (Figure 5) offers a clear depiction of the magnetic anomalies after adjustments were made for the Earth's magnetic field inclination and declination. This map was produced using a field average inclination of -17.01° and a field average declination of -3.2° . The total magnetic field intensity of the area ranged from 31,000nT to 34,000nT, with an average intensity of 32,425nT.

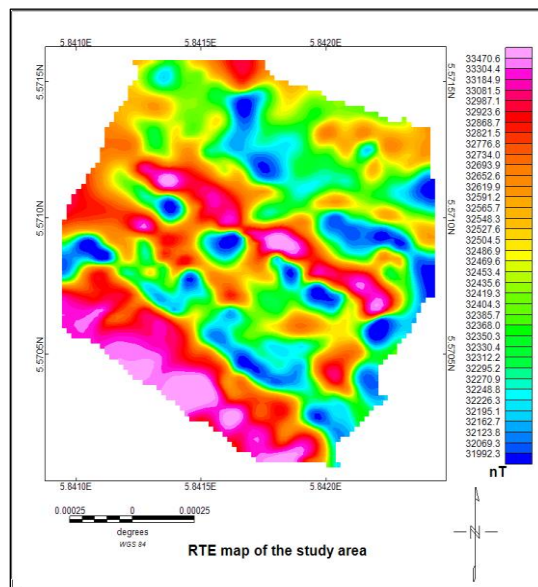


Figure 4 Reduction to Equator map of the study area

4.2. Upward Continuation Map

Figure 6 shows the total magnetic field intensity of the area after the data has been upward continued to 5m above the ground. The map helps to highlight deeper geological features while reducing the influence of near-surface noise, hence providing a clearer image of the magnetic anomaly which can be seen in the central area of the study area.

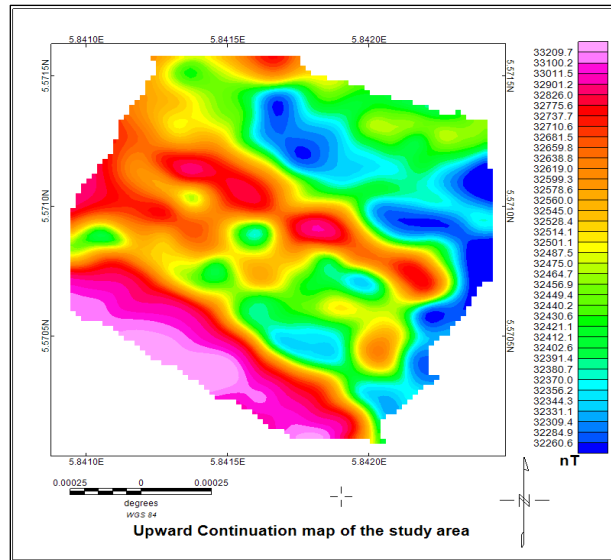


Figure 5 Upward Continuation map of the study area

4.3. First Vertical Derivative Map

The first vertical derivative of the study area's magnetic field intensity is displayed in Figure 7. With the help of the FVD map, which improves the high-frequency components of the magnetic data, near-surface geological structures may be seen more clearly. Small-scale features that might not be seen in the RTE or analytical signal maps are especially well highlighted by this map. The purple to red colours indicate points with a high positive change in the magnetic field while the blue to cyan colours indicate areas with a strong negative change in the magnetic field. These strong positive and negative changes highlight the presence of shallow sources in the area.

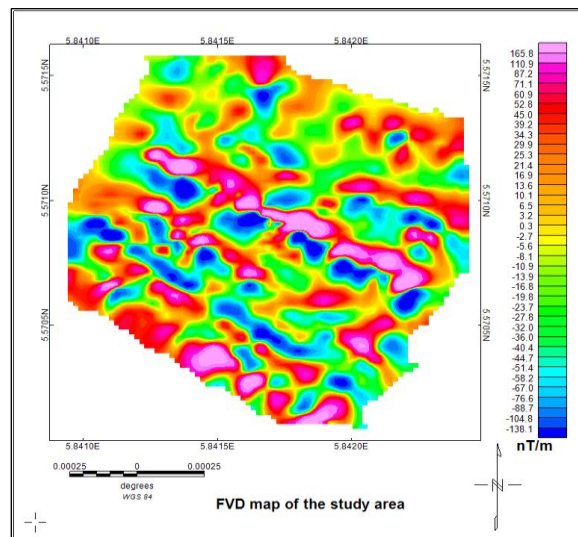


Figure 6 First Vertical Derivative map of the study area

4.4. Standard Deviation Map

The standard deviation map (figure 8) was created to delineate the edges of magnetic sources. By computing the statistical measure of the dispersion or spread of the magnetic field values. It's used to assess the variability in the magnetic data in both the x and y directions from the mean magnetic field, the map highlights areas of high magnetic deviations, often corresponding to geological structures such as dykes, sills, faults or lithological contacts.

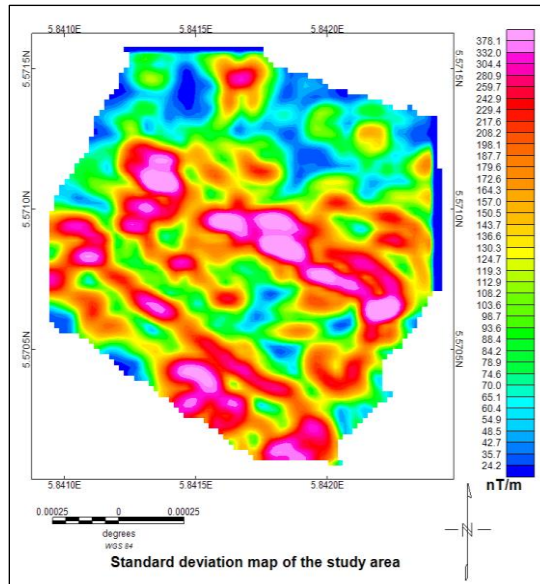


Figure 7 Standard deviation map of the study area

4.5. Source Parameter Imaging

The research area's Source Parameter Imaging (SPI) map, shown in Figure 9, shows the depth to the top of subsurface magnetic sources. The colour spectrum used on the map designates various depth levels using distinct hues. The values of yellow, green, and cyan correlate to increasingly deeper values, with light blue and blue representing the deepest sections, reaching depths of around 4000m to 5400m. Purple and red, on the other hand, show the shallowest depths (about 1000m to 1500m).

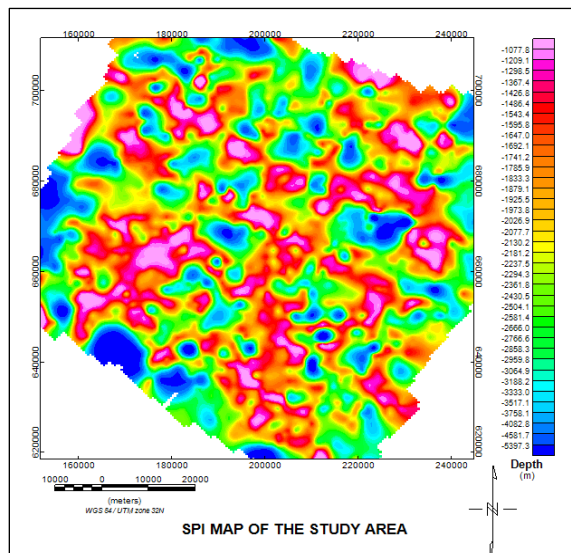


Figure 8 SPI map of the study area

4.6. Standard Euler Deconvolution

The Euler deconvolution maps indicate the derived source positions represented as circles at the located depths with colours indicating the depth ranges, while the clustering indicates the correct index. Figures 10 to 13 show the colour range symbol and colour range legend base maps for structural indices of 0, 1, 2 and 3 respectively for the residual field of the study area, while Table 2 shows a summary of the results.

For the Euler solutions map with a structural index of 0 (figure 10) which models contacts, the estimated sedimentary thickness and depths to the basement of the area ranges between 1,400m to 3,700m

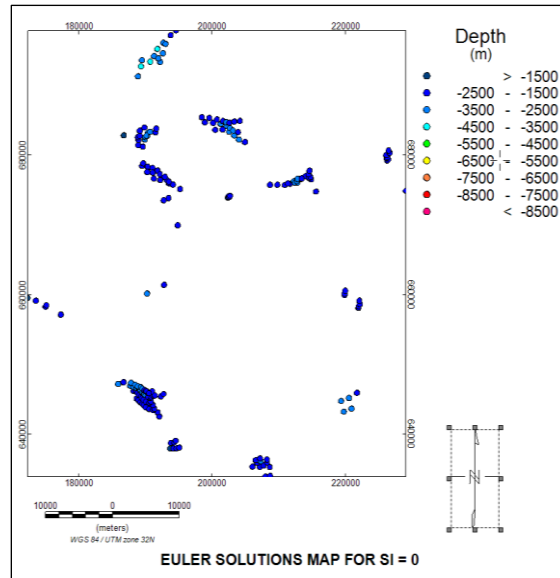


Figure 9 Euler Solutions Map for SI=0

For the Euler solutions map with a structural index of 1 (figure 11) which models dyke-like structures, the estimated sedimentary thickness and depths to the basement of the area range between 1,200m to 4,700m

For the Euler solutions map with a structural index of 2 (figure 12) which models pipe and horizontal cylinder structures, the estimated sedimentary thickness and depths to the basement of the area range between 2,300m to 6,700m.

For the Euler solutions map with a structural index of 3 (figure 13) which models spherical structures, the estimated sedimentary thickness and depths to the basement of the area range between 3,500m to 9,200m.

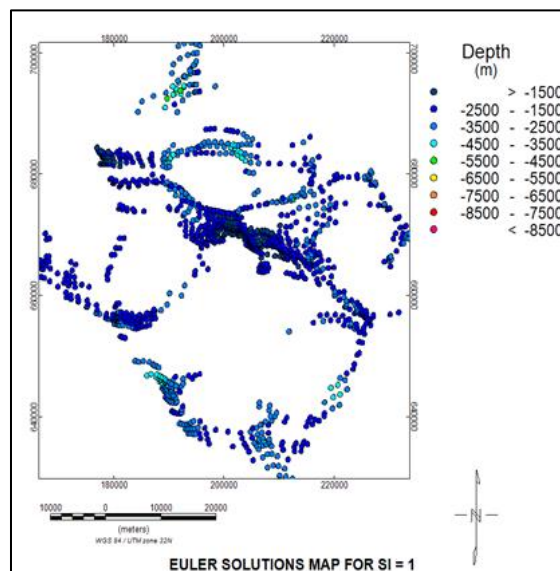


Figure 10 Euler Solutions Map for SI=1

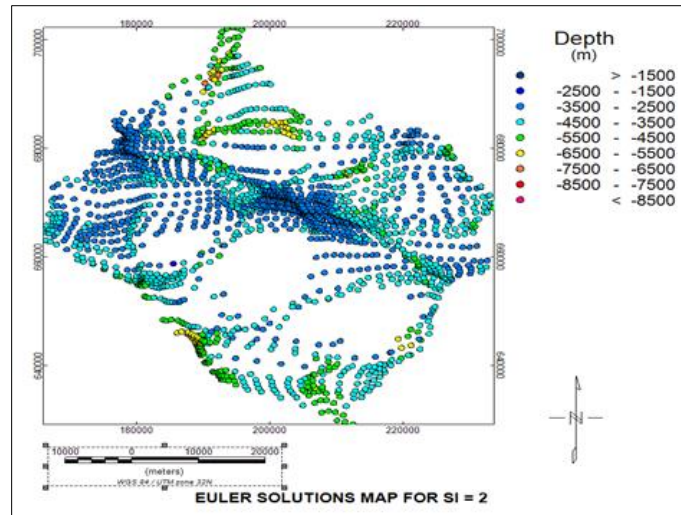


Figure 11 Euler Solutions Map for SI=2

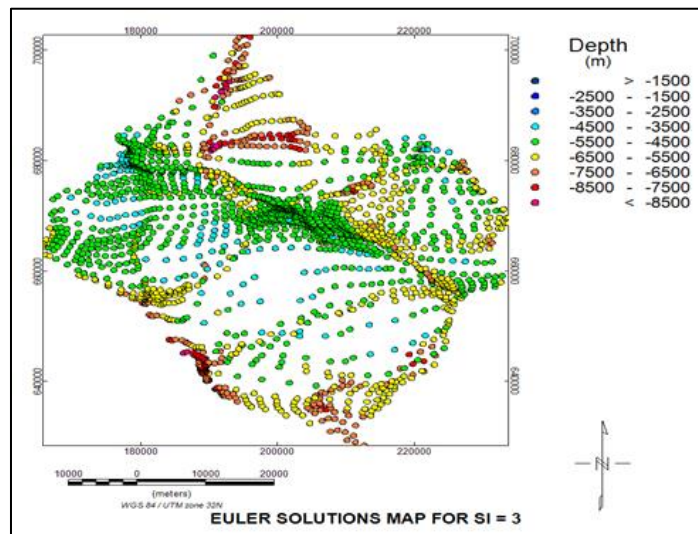


Figure 12 Euler Solutions Map for SI=3

Table 2 Estimated sedimentary thickness and depths to the basement in the study area.

S/N	Model	Approximate basement depth (m)
1	Source Parameter Imaging	1,000 – 5,400
2	Euler (structural index = 0)	1,400 – 3,700
3	Euler (structural index = 1)	1,200 – 4700
4	Euler (structural index = 2)	2,300 – 6,700
5	Euler (structural index = 3)	3,500 – 9,200

5. Discussion

The analysis of ground magnetic field data from the Niger Delta Basin, utilizing methods such as Reduction to Equator (RTE), First Vertical Derivative (FVD), and Upward Continuation (UC), has provided valuable insights into the basin's

subsurface structure, particularly concerning basement depth estimation. The RTE map revealed magnetic field intensity values ranging from 31,000nT to 34,000nT, suggesting lithological variations and structural differences across the area. These variations likely correspond to geological features such as faults and basement rock changes. Additionally, the FVD and UC maps revealed a prominent NW-SE magnetic anomaly, aligning with the known tectonic trends in the Niger Delta Basin, indicating the presence of significant subsurface features such as faults or basement edges.

Depth estimates derived from the Source Parameter Imaging (SPI) and Euler Deconvolution methods highlighted a complex basement topography, with SPI indicating basement depths ranging from 4,000 to 5,400 meters and shallow sources between 1,000 and 1,500 meters. Euler Deconvolution provided a broader depth range, with basement depths between 4,000 and 9,200 meters and shallow sources between 1,200 and 2,500 meters. These results suggest significant subsurface geological variability, potentially indicating uplifted or subsided areas and critical for understanding hydrocarbon migration and basin evolution. The combined use of these techniques offers a comprehensive understanding of the Niger Delta's subsurface geology, contributing to hydrocarbon exploration and the basin's geotectonic framework.

6. Conclusion

This study utilized ground magnetic field data to estimate basement depths in the Niger Delta Basin using Euler-3D deconvolution and Source Parameter Imaging (SPI) methods. The Reduced to the Equator (RTE) map revealed varying magnetic intensities. In contrast, the First Vertical Derivative (FVD) and Upward Continuation (UC) maps identified a prominent NW-SE magnetic anomaly, likely related to subsurface faults or fractures. SPI estimated basement depths between 4,000 to 5,400 meters and shallow sources at 1,000 to 1,500 meters, while Euler deconvolution provided a broader depth range of 4,000 to 9,200 meters, with shallow sources between 1,200 to 2,500 meters. The results from both methods align, offering a comprehensive understanding of the subsurface structure, crucial for hydrocarbon exploration and resource assessment.

Compliance with ethical standards

Acknowledgments

We acknowledge the Editor-in-chief and the Reviewers for their selfless services in improving this research work.

Disclosure of conflict of interest

We declare that there is no conflict of interest.

References

- [1] Asielue, K. O., Ugwu, G. Z., & Ikeh, J. C. (2019). Estimation of sedimentary thickness using spectral analysis of aeromagnetic data over Otukpo and Ejekwe areas of the lower Benue Trough, Nigeria. *International Journal of Physical Sciences*, Vol. 14(6), pp. 45-54. DOI: 10.5897/IJPS2019.4794
- [2] Avbovbo, A. A. (1978). Geothermal gradients in the southern Nigerian basin. *Bulletin Canadian Petroleum Geology*, v. 26(2), p. 268 – 274.
- [3] Avbovbo, A. A., & Orife, J. M. (1982). Stratigraphic and unconformity traps in the Niger Delta. *American Association of Petroleum Geologists, Bulletin*, v. 65, 251-265.
- [4] Biswas, A. (2017). Inversion of source parameters from magnetic anomalies for mineral /ore deposits exploration using global optimization technique and analysis of uncertainty. *Natural Resources Research*, 27(1), 77-107.
- [5] Burke, K. (1972). Longshore drift, submarine canyons, and submarine fans in development of Niger Delta. *American Association of Petroleum Geologists Bulletin*, v. 56, p. 1975 – 1983.
- [6] Cohen, H. A., & McClay, K. (1996). Sedimentation and Shale tectonics of the north-western Niger Delta front. *Marine and Petroleum Geology*, v. 13, p. 313 – 328.

- [7] Corredor, F., Shaw, J. H., & Bilotti, F. (2005). Structural styles in the deep-water fold and thrust belts of the Niger Delta. *American Association of Petroleum Geologists Bulletin*, v. 89, p. 753 – 780.
- [8] Dean, W. C. (1958). Frequency Analysis for Gravity and Magnetic Interpretation. *Geophysics*, Vol. XXIII (No. 1), Pp. 97-127.
- [9] Doust, H., & Omatsola, E. (1990). Niger Delta. in J.D. Edwards, and P.A. Santogrossi, eds., *Divergent/passive margin basins: American Association of Petroleum Geologists Memoir*, v. 48(p. 201 – 238).
- [10] Geosoft. (2006). "Euler Deconvolution Help" version 6.3
- [11] Heinio, P., & Davies, R. J. (2006). Degradation of compressional fold belts: Deep-water Niger Delta. *AAPG Bulletin*, v. 90, p. 753 – 770.
- [12] Hussaini, A., Idi, B. Y., Ndikilar, C. E., Nasir, M. M., Alhassan, A., Bala, N., Ibrahim, A., Yakubu, N., & Ayuba, I. (2021). Determination of Depth to Basement Using Spectral Analysis of Aeromagnetic Data over Azare Segment of Chad Basin. *Dutse Journal of Pure and Applied Sciences*, Vol. 7(No. 4b), 189-202. <https://dx.doi.org/10.4314/dujopas.v7i4b.20>
- [13] Johnson, E. A. E. (1998). Gravity and magnetic analyses can address various petroleum issues. Geologic applications of Gravity and Magnetic: case Histories. In *SEG Geophysical Reference No.8 and AAPG Studies in Geology* (No. 43 ed., pp. 7-8). I. Gibson., & P. S. Millegan. <http://dx.doi.org/10.1190/1.1437844>
- [14] Kasidi, S., & Nur, A. (2013). Spectral Analysis of Magnetic Data over Jalingo and Environs North – Eastern Nigeria. *International Journal of Science and Research (IJSR)*, 2(2), 448-454.
- [15] Li, X. (2008): Magnetic reduction-to-the-pole at low latitudes. Fugro Gravity and Magnetic Services. Houston, USA. Fugro
- [16] Meyer Jr, J. F. (1998). The compilation and application of aeromagnetic data for hydrocarbon exploration in interior Alaska. Geologic applications of Gravity and Magnetic: case Histories. In *SEG Geophysical Reference No.8 and AAPG Studies in Geology* (No. 43 ed., pp. 37-39). I. Gibson., & P. S. Millegan.
- [17] Morgan, R. (2004). Structural controls on the positioning of submarine channels on the lower slopes of the Niger Delta., in R.J. Davies, J.A. Cartwright, S.D Stewart, M. Lappin, and J.R. Underhill, eds., *3 D seismic technology: Application to the exploration of sedimentary basins: Geological Society (London) Memoir*, v. 29, p. 45 – 51.
- [18] Nettleton, L. I. (1954). Regionals, residuals, and structures. *Geophysics*, v. 19, p. 10-22.
- [19] Okiwelu, A. A., Ofrey-Kulo, O., & Ude, I. A. (2013). Interpretation of Regional Magnetic Field Data Offshore Niger Delta Reveals Relationship between Deep Basement Architecture and Hydrocarbon Target. *Earth Science Research*, Vol. 2(No. 1), 13 - 32. doi:10.5539/esr.v2n1p13
- [20] Pochat, S., Gumiaux, C., Castelltort, S., Besnard, K., & Vanden Driessche, J. (2004). A simple method of determining sand / shale ratios from seismic analysis of growth faults: An example from Upper Oligocene to Lower Miocene Niger Delta deposits. *American Association of Petroleum Geologists Bulletin*, v. 88, 1357 – 1367.
- [21] Reeves, C. (2005). "Aeromagnetic surveys: Principles, Practice and Interpretation," Geosoft Incorporated, Toronto Ontario, Canada.
- [22] Reid, A.B., Allsop, J.M., Granser, H., Millet, A.J. and Somerton, I.W. (1990). "Magnetic Interpretation in Three Dimensions using Euler Deconvolution". *Geophysics*, vol. 55, pp. 80-90.
- [23] Swartz, C. A. (1954). Some geometrical properties of regional maps. *Geophysics*, v. 19, p. 4.
- [24] Thomas, D. (1995). Exploration gaps exist in Nigeria's prolific delta. *Oil and Gas Journal*, p. 66 – 71.
- [25] Tsepav, M. T., & Mallam, A. (2017). Spectral Depth Analysis of some Segments of the Bida Basin, Nigeria, using Aeromagnetic Data. *J. Appl. Sci. Environ*, Vol. 21(7), 1330-1335. DOI: <https://dx.doi.org/10.4314/jasem.v21i7.19>
- [26] Whiteman, A. J. (1982). Nigeria. *Its Petroleum Geology, Resources and Potential: vols. 1 and 2: London, Graham and Trotman, Ltd*, 176p. and 238p., respectively.